

ARTICLE OPEN



Performance fluctuations and evaluation of a piston type integrated high pressure pump-energy recovery device

Yin Zhang ^{1,2}, Daiwang Song ^{1,2✉}, Haitao Wang ¹, Xiaoli Wang ¹, Lidong Jiang ¹, Chengpeng Wang¹, Man Fan ³ and Jingzhou Zhao ²

The development of energy recovery device (ERD) is a decisive factor for the recent prevalence of reverse osmosis (RO) technology in the seawater desalination field. Unlike broadly studied large scale ERDs, the investigations of small scale ERDs are scarcely reported, especially on the performance fluctuations under variable operating conditions. Based on an authors' exploratory research on a piston type integrated high pressure pump-energy recovery device (HPP-ERD), further performance exploitation of the HPP-ERD is conducted. With a constructed experiment platform, the influences of inlet seawater temperature, inlet seawater salinity, as well as the operating frequency on the performance of the HPP-ERD coupled with seawater reverse osmosis (SWRO) desalination system are investigated. The temperature and salinity of the inlet seawater are numerically correlated with the specific energy consumption (SEC) of the HPP-ERD. With the correlated equation, the marine hydrological data of two observatories acquired from a national authoritative database, and the annualized life cycle cost approach incorporated, annual performance assessment is proposed for an SWRO desalination system equipped with the HPP-ERD in the light of energy and economic indices. The study results indicate that the proposed HPP-ERD is competent under various operating conditions for SWRO desalination systems.

npj Clean Water (2022)5:19; <https://doi.org/10.1038/s41545-022-00162-5>

INTRODUCTION

The world is faced with exacerbated water scarcity problem as a consequence of accelerated global industrialization, urbanization, and population growth^{1–4}. Seawater desalination is one of the most promising method to provide clean and drinkable water for the global population, alleviating the water shortage crisis of coastal countries and regions^{5–8}. Among various desalination technologies, the reverse osmosis (RO) has taken a dominating role throughout the seawater and brackish water desalination market because of its simplicity in operation and low energy demand^{9–12}. At present, RO technology is used in 84% of the overall operating desalination plants in the world and these RO-based plants contribute 69% to the global desalination water production¹³.

In retrospect of the development history of RO technology, the emergence and prevalence of energy recovery device (ERD) is widely regarded as the most critical factor that attributes to the domination of RO in the seawater desalination market^{14,15}, because the energy consumption of RO process can be reduced by over 50% with the adoption of ERDs^{16–18}. Typical commercialized ERDs which are still popular up to date include Turbocharger^{19–21}, DWEER²², PX^{20,22–24}, iSave^{25,26}, and RO Kinetic²⁷, all of which have been meticulously studied and thoroughly introduced. It is noteworthy that these types of ERDs are mostly utilized in medium and large-scale SWRO plants. The specifications of these medium to large-scale ERDs are summarized in Table 1 according to their official brochures.

From the practical view, equipping ERD is not the favored alternative for most small-scale SWRO projects^{28–30}, which can be ascribed to the unaffordable capital cost, complex installation demands, and professional operating principles of small scale ERDs. Therefore, performance of ERDs for small scale SWRO are

basically reported in laboratory, prototype or pilot related literatures, such as the integration of Axial Piston Pump (APP) and Axial Piston Motor (APM) of Danfoss^{31–33}, the Clark pump of Spectra Watermakers Inc.^{33–36}, the incorporation of water vane pump and hydraulic vane motor of Xi'an Jiao Tong University³⁷, as well as the self-boosting energy recovery device (SB-ERD) and the three-cylinder energy recovery device (TC-ERD) of Tianjin University^{38,39}. The vital characters of these small-scale ERDs are remarked in Table 2, which are collected from the mentioned literatures or their brochures.

For SWRO projects, the RO separation performance and fluid flow balance are susceptible to the fluctuations of ambient seawater parameters⁴⁰. Practical large-scale SWRO projects can adjust to the inlet situation fluctuations and device failures easily by controlling the number of actual operating driving devices, such as the Tuas Seawater Desalination Plant in Singapore⁴¹. For small-scale SWRO projects equipped with few ERDs, the system performance under unsteady conditions relies on the operation characteristic of the ERD itself to a great extent. However, very few studies have discussed the performance fluctuations of a single ERD under variable operating circumstances yet.

In terms of variable flowrates, Zhou et al.⁴⁰ investigated the capacity flexibility of a reciprocating- switcher energy recovery device whose design capacity is 30 m³ per hour. The actual capacity was observed to range between 66.7% and 150.0% of the nominal value from the experiments while high and steady efficiency was maintained. The transient performance of PX under both laboratory circumstance and practical operating conditions of Hamma desalination plant in Algeria⁴² was explored. The research data indicated that PX could accommodate the unsteady inlet flows from the hydraulic safety aspect. The practical operating data of PX under various lead flow conditions in the

¹The Institute of Seawater Desalination and Multipurpose Utilization, MNR (Tianjin), Tianjin 300192, PR China. ²Tianjin Blue Cross Membrane Technology Co., Ltd, Tianjin 300192, PR China. ³School of Energy and Environmental Engineering, Hebei University of Technology, Tianjin 300401, PR China. ✉email: songdw123@126.com

Table 1. The specifications of several kinds of medium to large-scale ERDs.

Name	Manufacturer or inventor	Processing flowrate (m ³ per hour)	Energy-saving performance
AT Turbocharger	ERI	11–2272	Not given
HPB Turbocharger	FEDCO	10–2800	Efficiency: up to 84%
DWEER	Flowserve	Up to 350	Efficiency: up to 98%
PX	ERI	4.5–68.1	Peak efficiency: 96–98%
iSave	Danfoss	6–70 (in terms of high-pressure outlet)	Energy-saving percentage: 60% (for iSave 21 Plus)
RO Kinetic®	Manuel Barreto	625–5263 (derived indirectly from ref. 27)	Maximum efficiency: 98%

Dhekelia Desalination Plant, Cyprus suggested that the lubrication flow was barely affected by the variation of the lead flow, while the energy consumption decreased at larger lead flow values⁴³.

The feed seawater temperature is another important factor which might cause the HPP and ERD performance variations of RO projects. It was forecasted by Koutsou et al.⁴⁴ that with the feed-water temperature increasing from 15 °C to 40 °C, the HPP efficiency was escalated just by 1% for both seawater and brackish water, while the corresponding ERD (ERI “PX-Q300”) efficiency was reduced by 0.75% and 8.8% for seawater and brackish water cases, respectively. The operating data of several SWRO plants in Saudi Arabia was collected⁴⁵. It was found out that in Yanbu Plant and Duba Plant, the temperature variation of feed seawater (25–35 °C for Yanban and 24–30 °C for Duba) had insignificant impact on the ERD performance.

The present study focuses on the operating characteristics of a piston type integrated high pressure pump-energy recovery device (HPP-ERD). Its operating principle, laboratory test results of three types of prototypes, and 1-month practical operation conditions of one of the prototypes have been introduced in the authors’ previous work⁴⁶. Based on the previous research consequences, the present paper introduces the subsequent research which further explores the performance fluctuations of the HPP-ERD coupled with SWRO desalination system in terms of various operating parameters. The annual performance simulation of the HPP-ERD under actual circumstance parameters is also implemented. To meet the boosting demand of small-scale seawater desalination plants^{28,47}, the proposed paper aims to discover the adaptability of the HPP-ERD in terms of diverse operating situations, and further prove its feasibility in small scale SWRO projects.

RESULTS AND DISCUSSION

Three sets of tests are executed in August 2021 in Tianjin, China to discuss the impacts of key parameters on the system fresh water productivity, freshwater salinity, recovery ratio (RR) and SEC. The definitions of RR and SEC are given in Eqs. (1) and (2), separately.

$$RR = \frac{Q_{fw}}{Q_{sw,feed}} * 100\% \quad (1)$$

$$SEC = \frac{W_{ele}}{Q_{fw}} \quad (2)$$

where Q_{fw} denotes the fresh water productivity, $Q_{sw,feed}$ denotes the feed seawater flowrate, W_{ele} denotes the electricity energy consumption rate and the energy-related unit of the present study, such as kW·h, refers to the electricity consumption.

The effects of inlet seawater temperature

The univariate variable, namely the feed seawater temperature, is designed as 5.0 °C, 10.0 °C, 15.0 °C, 20.0 °C, 25.0 °C, 30.0 °C, and 35.0 °C, respectively. During the test period the biggest deviation between the detected feed seawater temperature and the designed value is no more than 0.2 °C for each condition. The

effects of feed seawater temperature on the system fresh water productivity, fresh water salinity, RR, and SEC are described in Fig. 1a.

As for the RR, it ranges from 39.7 to 40.2% for the seven operating conditions and its average value is 39.9%. Thus, it is apparent that the RR can be kept at a highly steady value with varying feed seawater temperature.

Meanwhile, the salinity of the fresh water increases from 0.235 psu to 0.438 psu as the feed seawater temperature increases from 5.0 °C to 35.0 °C. The enhanced salinity can be attributed to the separation performance deterioration of the RO membrane under high ambient seawater temperatures. Specifically, the separation performance deterioration of the RO membrane refers to the enlargement of membrane pores and naturally leads to the less pure fresh water and pressure reduction of the processed seawater before entering the RO membranes.

On the fact that the overall seawater volume within a certain time interval pumped by the HPP-ERD is barely changed with constant operating frequency, the processing seawater flowrate is nearly constant as the feed seawater temperature increases from 5.0 °C to 35.0 °C. Comprehensively considering the relevantly constant feed seawater flowrate and RR, the fresh water productivity also fluctuates within a very narrow scope. The average fresh water productivity is ~1.95 m³ per hour and the corresponding deviation between the individual and the average is <2.5%.

Since the fresh water productivity and RR are insusceptible to the feed seawater temperature, the SEC declines from 3.56 kW·h per m³ to 2.73 kW·h per m³ by 23.3% with the feed seawater temperature escalated from 5.0 °C to 35.0 °C as a consequence of separation performance deterioration of the RO membrane.

The effects of inlet seawater salinity

The inlet seawater salinity represents the overall quality of feed seawater. The univariate variable, namely the feed seawater salinity is designed as 21.0 psu, 24.5 psu, 28.0 psu, 31.5 psu, 35.0 psu, and 38.5 psu, respectively. During the test period, the largest deviation between the detected value and the designed value in terms of the feed seawater salinity is 0.571% among all the operating conditions. The effects of salinity on the system fresh water productivity, fresh water salinity, RR, and SEC are described in Fig. 1b.

As for the RR, it ranges from 39.4 to 40.3% for the six operating conditions and its average value is 39.8%. It is obvious that the feed seawater salinity has trivial impact on the RR, which is analogous to the feed seawater temperature.

The processing seawater flowrate is also stable for Set B with constant operating frequency. Linking with steady RR, the fresh water productivity ranges from 1.94 m³ per hour to 1.99 m³ per hour with an average value of 1.96 m³ per hour.

Meanwhile, the growth of salinity of the fresh water can be easily anticipated and understood if the feed seawater salinity is escalated. Specifically, the fresh water salinity grows from

Table 2. The characters of several kinds of small-scale ERDs.

Name	Manufacturer or inventor	Production flowrate	Energy-saving performance
APP-APM	Danfoss	0.3–0.82 m ³ per hour (for two-hole electric motor)	SEC: 3–3.5 kW·h per m ³ (for 50 bar operating pressure)
Spectra Clark Pump Intensifier	Spectra Watermakers	24–156 LPH	Rated SEC: 3.96–4.76 kW·h per m ³ (derived indirectly from brochure)
Integration of pump and hydraulic motor	Xi'an Jiao Tong University	0.36–2.06 m ³ per hour	SEC: 6.2–10.4 kW·h/m ³ (for 42 bar operating pressure)
SB-ERD	Tianjin University	4.38–4.84 m ³ per hour (derived indirectly from ref. ³⁸)	Efficiency: 91.55–92.41%
TC-ERD	Tianjin University	20–35 m ³ per hour	Efficiency: 95.9–98.2%

0.270 psu to 0.483 psu as the feed seawater salinity increases from 21.0 psu to 38.5 psu.

On the other hand, the increment of feed seawater salinity inevitably leads to higher operating pressure of the HPP-ERD to separate the higher concentration of salt and pure water, and necessarily brings larger energy consumption. The SEC increases gradually from 2.33 kW·h per m³ to 3.66 kW·h per m³ by 57.1% with the feed seawater salinity escalated from 21.0 psu to 38.5 psu.

The effects of operating frequency

For the univariate variable, namely the operating frequency is designed and kept as 30 Hz, 35 Hz, 40 Hz, 45 Hz and 50 Hz, respectively. The upper limit of the operating frequency is designed to be 50 Hz, which is the standard frequency for residential and industrial electricity grid of China. Frequency over 50 Hz is not considered to avoid unnecessary capacity redundancy of the device. The lower limit of the operating frequency is chosen as 30 Hz because the RO membrane surface will suffer from the risk of being partially moistened and damaged with the operating frequency <30 Hz. The effects of operating frequency on the system fresh water productivity, fresh water salinity, RR, and SEC are described in Fig. 1c.

As for the RR, it ranges from 39.6 to 40.9% for the five operating conditions and its average value is 40.4%. It can be clearly seen that the operating frequency has minor influence on the RR as well.

The reduction tendency of the fresh water productivity is easily expected. An approximate linearity relationship between the fresh water productivity and the operating frequency can be observed from Fig. 1c. The fresh water productivity is enhanced from 1.235 m³ per hour to 2.221 m³ per hour as the operating frequency increases from 30 Hz to 50 Hz.

The salinity of the fresh water tends to increase as the operating frequency decreases. It is boosted from 0.357 psu to 0.428 psu by 19.9% as the operating frequency declines from 50 Hz to 30 Hz. The influence of operating frequency on fresh water salinity is less significant compared with the inlet seawater temperature and inlet seawater salinity.

The SEC increases from 2.76 kW·h per m³ to 5.90 kW·h per m³ by 113.8% with the reduction of operating frequency from 50 Hz to 30 Hz. Polynomial regression is attempted to describe the relationship between the SEC and operating frequency. A quadratic polynomial relationship is found to be adequate with the *R* square value of 0.9998 proving its high accuracy. The quadratic polynomial relationship is written in Eq. (3) and the curve-fitting result is portrayed in Fig. 2.

$$SEC = 0.0101 * (f)^2 - 0.962 * f + 25.681 \quad (3)$$

The increasing tendency of SEC is more obvious for small operating frequency scenarios. The characteristic of the proposed HPP-ERD that device efficiency drops dramatically with gradual

deviation of operating frequency from the rated value is similar to the characteristic of typical piston type pumps⁴⁸.

Annual performance prediction of the HPP-ERD

Annual performance evaluations from both energy and economic aspects are conducted for rated operating frequency condition to further explore the annual performance of the proposed HPP-ERD coupled with SWRO system. The prediction is undertaken based on the numerical correlations in terms of the SEC, as well as the authoritative marine hydrological data of two observatories in China.

Conforming to the abovementioned results of the current study and broadly recognized physical principles, several assumptions are proposed for the performance evaluation:

- (1) The prediction is undertaken for the rated operating frequency of 45 Hz.
- (2) The RR is assumed to be 40%.
- (3) The feed seawater flowrate has the linear relationship with the operating frequency.
- (4) The fresh water quality is assumed to be eligible.
- (5) The desalination system is presumed to be operated consecutively each day.

Combining the assumptions and the marine hydrological data, the daily SECs of the HPP-ERD for the two observatories are calculated and illustrated in Fig. 3.

The SEC_{HPP-ERD} ranges from 3.020 kW·h per m³ to 3.531 kW·h per m³ for the Shidao Observatory scenario and ranges from 2.308 kW·h per m³ to 3.349 kW·h per m³ for the Lianyungang Observatory scenario. The corresponding annually average values of SEC_{HPP-ERD} for the Shidao Observatory scenario and Lianyungang Observatory scenario are 3.310 kW·h per m³ and 3.026 kW·h per m³ individually, which can be deemed satisfactory for such a small scale RO desalination device.

Furthermore, comprehensively considering the energy consumption of the HPP-ERD and other possible expenditures, the annual fresh water cost for the Shidao Observatory scenario and Lianyungang Observatory scenario are computed to be 0.927 USD per m³ and 0.903 USD per m³, separately. Considering a rough estimation of the shipping cost of fresh water of 1.89 USD per m³⁴⁶, the calculated annual fresh water costs hint the outstanding economic superiority of the HPP-ERD for sparsely populated islands.

Performance summary

Reviewing the consequences of abovementioned univariate laboratory tests, the main operating performance of the HPP-ERD can be outlined for three aspects, namely the fresh water salinity, the SEC, and the RR.

In terms of the fresh water salinity, it fluctuates from 0.197 psu to 0.483 psu for all the studied cases. The corresponding water quality suggested by the range of salinity is acceptable for

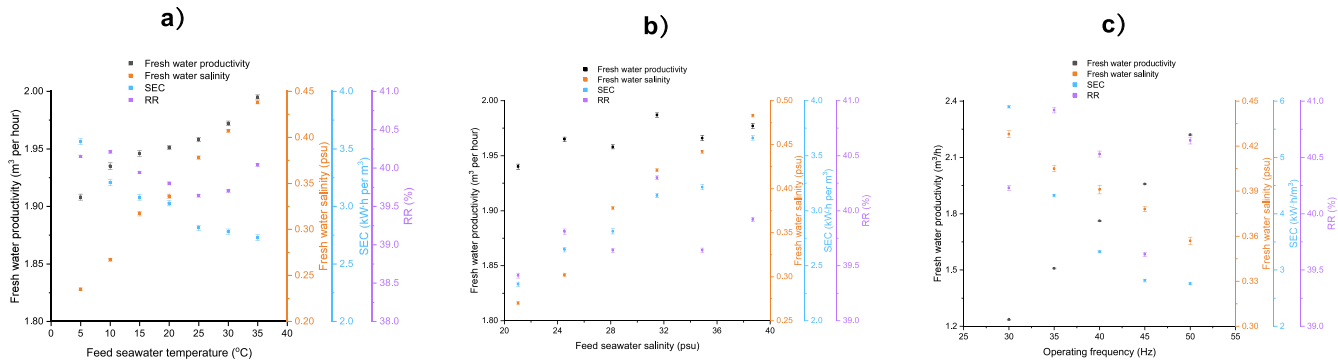


Fig. 1 System performance fluctuations under variable operating conditions. **a** The influences of feed seawater temperature on fresh water salinity, SEC of RO process and RR of RO system are portrayed. **b** The influences of feed seawater salinity on fresh water salinity, SEC of RO process and RR of RO system are portrayed. **c** The influences of operating frequency on fresh water salinity, SEC of RO process, and RR of RO system are portrayed. Error bars indicate the standard deviation.

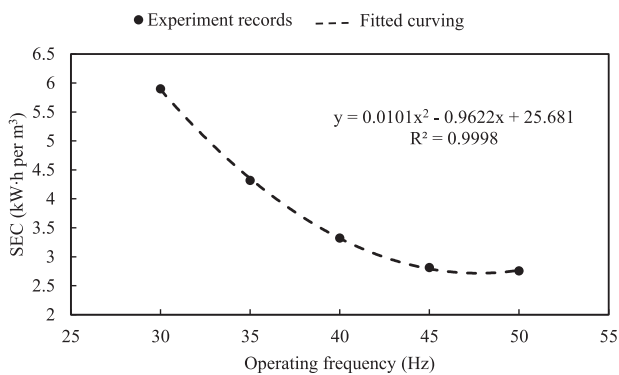


Fig. 2 The regressed relationship between the SEC and operating frequency. The quadratic polynomial relationship between the SEC and operating frequency with high credibility is delineated.

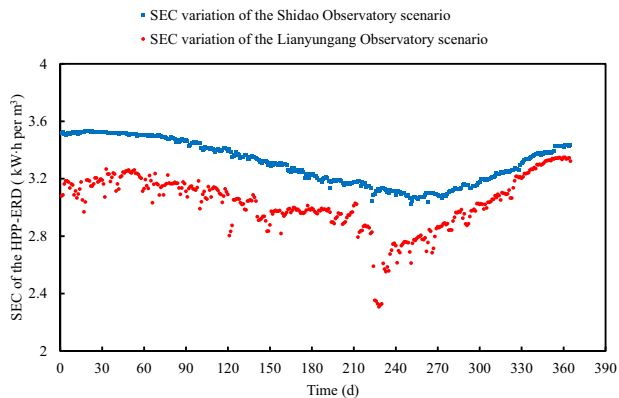


Fig. 3 Annual SEC variations of the HPP-ERD. Annual SEC variations of the HPP-ERD under the Shidao Observatory scenario and the Lianyungang Observatory scenario are plotted.

desalted water, which indicates that the proposed HPP-ERD can provide sufficient high pressure for the RO separation process under various conditions.

The SEC of the all the concerned scenarios ranges from 2.33 kW-h per m³ to 5.90 kW-h per m³. The authors concluded in the previous study⁴⁶ that the common range of SEC of small scale ERDs whose rated capacity is <50 m³ per day is ~2–6.2 kW-h per m³ under laboratory circumstances, according to various public literatures. Furthermore, very few ERDs have been adopted in small scale RO desalination projects^{28–30} and the literature

retrieval in Web of Science and Elsevier databases cannot find out the description of the SEC of small scale ERDs in practical SWRO projects except for the authors' previous study⁴⁶. Otherwise, the SEC of small SWRO systems unequipped with ERD is reported to exceed 10 kW-h per m³ and attains as much as 33 kW-h per m³ under unfavorable conditions^{36,49,50}. Hence, the SEC of the proposed HPP-ERD under various operating conditions is appreciable once applied in practical small scale SWRO projects to replace the stand-alone high pressure pump. Furthermore, it is also implied that, under temporary unfavorable circumstances such as insufficient seawater penetration of intake well and limited electricity supply, the proposed HPP-ERD is capable of producing fresh water firmly with acceptable energy consumption performance, if the operating frequency is adjusted to deviating from the rated value within a certain range.

For all the involved cases, the RR ranges between 39.4% and 40.9% with insignificant fluctuation. Piston pump belongs to the positive displacement type pump, whose flowrate has a linear relationship with the rotation speed. The proposed HPP-ERD is composed of one piston type high pressure pump and one energy recovery device which is essentially a reversely rotating piston type pump. Both the flowrates of the two components have the linear relationship with the rotation speed. As the high pressure pump and the energy recovery device are fabricated to the same shaft, they have the consistent rotation speed. Therefore, the flowrate ratio of them is theoretically constant. The flowrate of the high pressure pump is evidently the sum of fresh water flowrate and concentrated brine flowrate. Consequently, it can be asserted that the RR of the proposed HPP-ERD shall be constant as a result of its own mechanical characteristic. The lesser fluctuation of RR might be ascribed to the inevitable measurement uncertainty.

As for the economic aspect, annual performance evaluation shows that the fresh water cost for the Shidao Observatory scenario and Lianyungang Observatory scenario are 0.927 USD per m³ and 0.903 USD per m³, respectively, which are much cheaper than that of water transportation cost. It should be stressed that the fresh water cost reflects purely the economic superiority. For possible future research of the HPP-ERD in terms of life cycle energy efficiency or carbon emission, the electricity consumption shall be associated with the primary fossil fuel consumption through quantitative evaluation, for instance, the conversion factor reported by Ng et al.⁵¹.

In summary, the research consequences of the proposed HPP-ERD show prominent ability in low energy consumption, eligible fresh water quality, flexible compatibility, and economic superiority over conventional water transportation. In particular, the RR of the proposed HPP-ERD is constant under various operating conditions, which is convenient for the accurate preliminary design of the SWRO projects.

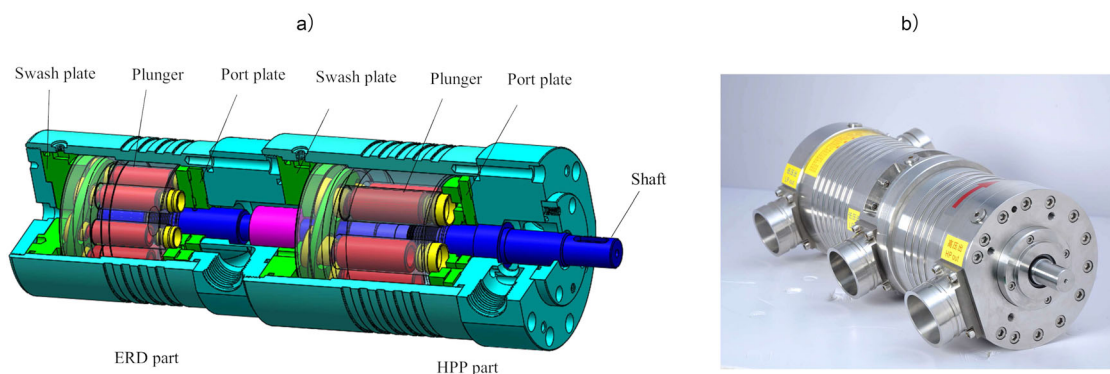


Fig. 4 Portrayal of the HPP-ERD. **a** Structure diagram (reprinted from ref. ⁴⁶, with permission from Elsevier) shows that the proposed HPP-ERD is mainly composed of swash plates, plungers, port plates, and one shaft. **b** The actual appearance of the proposed HPP-ERD prototype is given in the photograph.

METHODS

Brief introduction of the HPP-ERD

The HPP-ERD is a typical piston type of ERD patented by ISDMU (The Institute of Seawater Desalination and Multipurpose Utilization, MNR (Tianjin)) and Woer Technology Co., Ltd, which naturally belongs to the isobaric ERD category. As shown in Fig. 4a, the ERD part, high pressure pump (HPP) part and electric machinery constitute a completed HPP-ERD, and they are affixed in succession to a radical shaft with two bearings. Figure 4b is a photograph of one HPP-ERD prototype.

The plungers of the ERD part recover the hydraulic energy of the brine returning from the membrane module, and then deliver the energy to the HPP along the shaft. Actuated by both the electric machinery and the recovered hydraulic energy, the HPP pressurizes the low-pressure seawater to attain the high pressure for further reverse osmosis process. The concentrated brine rejected by the RO membranes flows to the ERD part and is finally discharged. It is noteworthy that the operating motor is a single-shafted machinery rather than usual double-shafted type to save the manufacture cost.

The fresh water productivity range of different HPP-ERD prototype versions is 0.246–2.166 m³ per hour (~5–50 m³ per day) and is thus, proper for small scale SWRO projects from the capacity facet. The thorough delineation of the HPP-ERD is reported in ref. ⁴⁶.

Experiment scheme

The prototype version of HPP-ERD with a rated fresh water productivity of 50 m³ per day is selected as the research target for the experiment. This capacity is popular in the small scale desalination market of China. In accordance with the aforementioned literature review, the feed seawater temperature ($t_{sw,feed}$), the feed seawater salinity ($S_{sw,feed}$), as well as the operating frequency (f) are determined as the three controlling variables of the proposed experiment to disclose the operating characteristics of the HPP-ERD. Three sets of univariate laboratory tests are scheduled for the temperature (Set A), salinity (Set B), and frequency (Set C), separately. Table 3 shows the expected designing parameters of all the experimental conditions and the univariate variables are labeled in bold.

The feed seawater temperature is designated to range between 5.0 °C and 35.0 °C, while the feed seawater salinity is designated to range between 21.0 psu and 38.5 psu. These two ranges are decided based on the abundant desalination design and operation experience of ISDMU, and can cover most of the possible seawater situations which may be encountered by the seawater desalination projects of China. The operating frequency is regulated from 30 Hz to 50 Hz through a variable frequency drive during the experiment period to explore the capacity flexibility of the prototype.

Under the abovementioned conditions, the crucial feed seawater parameters and system operating parameters are recorded every 20 s and its operating characteristics are meticulously analyzed. For each operating condition, the operating data of the initiation period is neglected and the average values of the recorded parameters of five-minute steady period are taken for the subsequent analysis.

Table 3. Designed details of the experimental conditions.

Condition NO.	$t_{sw,feed}$ (°C)	$S_{sw,feed}$ (psu)	f (Hz)
A1	5.0	28.0	45
A2	10.0	28.0	45
A3	15.0	28.0	45
A4	20.0	28.0	45
A5	25.0	28.0	45
A6	30.0	28.0	45
A7	35.0	28.0	45
B1	25.0	21.0	45
B2	25.0	24.5	45
B3 (A5)	25.0	28.0	45
B4	25.0	31.5	45
B5	25.0	35.0	45
B6	25.0	38.5	45
C1	25.0	28.0	50
C2 (A5)	25.0	28.0	45
C3	25.0	28.0	40
C4	25.0	28.0	35
C5	25.0	28.0	30

The univariate variables of the operating conditions are labeled in bold.

Experiment platform and instruments

A test platform is devised and established for the experiment scheme, the flow chart and photographs of which are portrayed in Fig. 5. The platform locates at Binhai District, Tianjin, China (39.1°N, 117.7°E), where the seawater from the nearby Bohai Sea can be easily acquired. The experiment platform complies with the following operating principle for a single test condition:

The circulating pump motivates the feed seawater to flow from the constant temperature water tank to the HPP-ERD inlet. The feed seawater is pressurized inside the HPP-ERD and pumped from the HPP part to the RO membrane module. The desalinated water leaving the RO membrane module is discharged to the tank, while the concentrated brine out of the RO membrane module returns to the ERD part of the HPP-ERD. The hydraulic energy of the brine is passed to the feed seawater and the low-pressure brine is emitted back to the tank as well.

The feed seawater is mixed by the actual seawater and pure water with a proper proportion which can assure that the feed seawater satisfies the presumed salinity values. The feed seawater temperature is controlled by the constant water tank. A variable frequency drive is installed to change the operating frequency of the HPP-ERD and further control the feed seawater flowrate. The two RO membrane modules in parallel in the platform are outfitted with the RO membranes produced by DOW Filmtec.

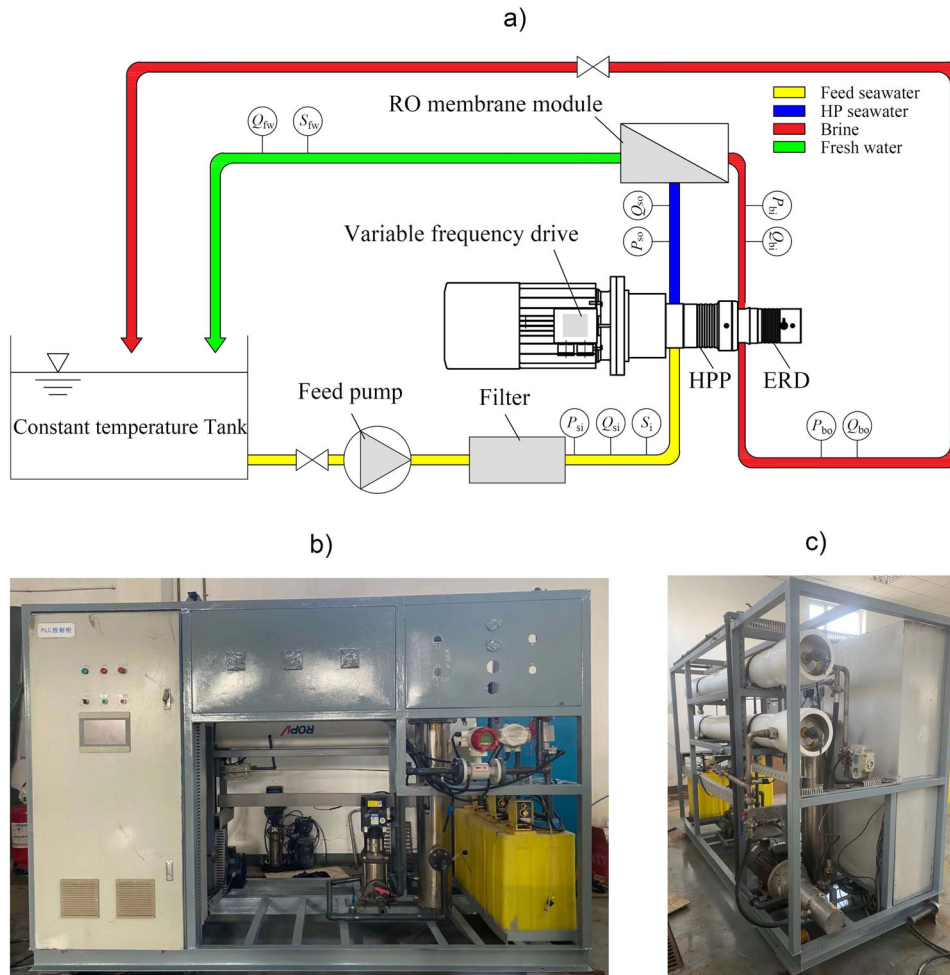


Fig. 5 Portrayal of the experiment platform. **a** Circulating loops of feed seawater, high pressure seawater, brine and fresh water are illustrated in the flow chart. The primary segments of the experiment platform are marked. **b** Photograph of the experiment platform from the front view. **c** Photograph of the experiment platform from the oblique view.

Since the experiment duration is very short compared with the membrane module lifespan, the impact of membrane scaling on the experiment results is assumed to be negligible. An integrated controller box is built to control the experiment process, exhibit and record all the experimental data.

Four manometers and five flowmeters are necessary for the proposed experiment platform. As tagged in Fig. 5a, P_{s1} , P_{s2} , P_{s3} , P_{s4} and P_{b1} , P_{b2} , P_{b3} , P_{b4} are the pressure (volumetric flowrate) measurands for the unpressurized feed seawater, the pressurized seawater entering the RO membrane modules, the concentrated brine returning to the ERD part and the concentrated brine discharged to the tank, separately. Additionally, Q_{fw} refers to the volumetric flowrate measurand for the fresh water. The recovery ratio (RR) can be readily computed from the directly measured volumetric flowrates. The electricity power of the HPP-ERD (W_{ele}) is documented through a wattmeter during the experiment period. Two salinity meters are placed to detect the salinities of the feed seawater and fresh water. The instruments to measure the introduced parameters are listed in Table 4.

Numerical correlation

The numerical correlation intends to correlate the SEC with the temperature and salinity of the feed seawater under the rated operating frequency (45 Hz). The experiment data of Set A and Set B are chosen as the regression sources. A linear regression relationship between the SEC and the two feed seawater parameters is discovered with the least square curve-fitting method. The regression result is expressed in Eq. (4). The adjusted R square value and the significance F value of the correlation are

Table 4. Instruments with accuracy, range, and standard uncertainty.

Instrument	Measured parameter	Accuracy	Range
Thermocouple	Temperature	0.1 °C	0–200 °C
Manometer	Water pressure	0.5%	0–1 MPa
Manometer	Water pressure	0.5%	0–10 MPa
Electromagnetic flowmeter	Fluid flowrate	0.5%	0.6–6 m ³ per hour
Wattmeter	Electricity power	10 W	0–10 kW
Salinity meter	Salinity	0.002 psu	0–2.5 psu
Salinity meter	Salinity	1%	0–42 psu

0.963 and 7.461×10^{-7} separately, which proves that the regression consequence is greatly convincing.

$$SEC = 1.422 - 0.0199 \times t_{sw,feed} + 0.0695 \times S_{sw,feed} \quad (4)$$

where SEC denotes the specific energy consumption under the operating frequency of 45 Hz, $t_{sw,feed}$ denotes the feed seawater temperature, $S_{sw,feed}$ denotes the feed seawater salinity. This correlation is valid within the feed seawater temperature range of 5.0–35.0 °C and the feed seawater salinity range of 21.0–38.5 psu.

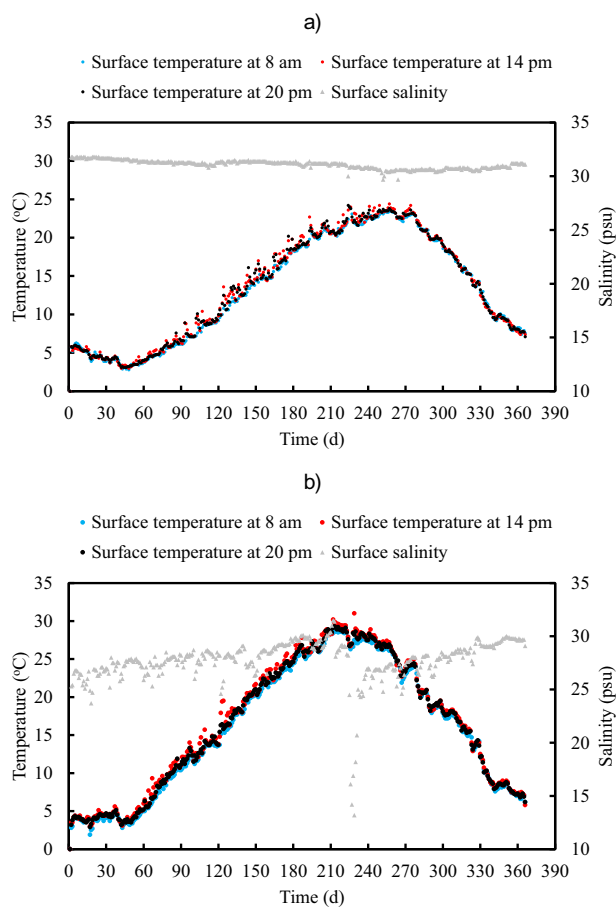


Fig. 6 Surface temperature and salinity records of the two observatories. **a** Data of Shidao Observatory, **b** Data of Lianyungang Observatory.

Acquisition, analysis, and disposal of marine hydrological data

The marine hydrological data are issued by the National Marine Data Center of China and can be accessed from its website address (<http://mds.nmdis.org.cn>). The annual marine hydrological data of 2019 in terms of salinity and temperature of surface seawater of Shidao Observatory, Shandong Province, China (36.9°N, 122.4°E) and Lianyungang Observatory, Jiangsu Province, China (34.8°N, 119.4°E) are collected from the database entitled "Temperature and salinity observation data in Chinese oceanic stations".

For both the observatories, the salinity is measured and documented once a day, while the temperature is measured and documented at 8 am, 14 pm, and 20 pm, respectively each day. The detailed measurement values from 1 January 2019 to 31 December 2019 are depicted in Fig. 6.

As Fig. 6 shows, the overall surface seawater temperature of Shidao Observatory is lower than that of Lianyungang Observatory. For the surface seawater temperature of Shidao Observatory, the average values at 8 am, 14 pm, and 20 pm, the maximum value of all the temperature measurands, and the minimum value of all the temperature measurands are 13.3 °C, 13.7 °C, 13.6 °C, 24.4 °C, and 2.8 °C individually. The counterparts of Lianyungang Observatory are 16.0 °C, 16.6 °C, 16.3 °C, 31.0 °C, and 1.9 °C individually.

Figure 6 also suggests that the overall surface seawater salinity of Shidao Observatory is higher than that of Lianyungang Observatory. For the surface seawater salinity of Shidao Observatory, the average value, maximum value, and the minimum value of all the salinity measurands are 31.1 psu, 31.8 psu, and 29.7 psu individually. The counterparts of Lianyungang Observatory are 27.7 psu, 31.5 psu, and 13.2 psu individually.

The daily fluctuations of surface seawater temperature at the two observatories are both moderate. The maximum daily fluctuation of the three detected temperatures of any single day is 2.9 °C for Shidao Observatory and 4.0 °C for Lianyungang Observatory. The fluctuation of

surface seawater salinity at Shidao Observatory is mild. The maximum salinity fluctuation of any two consecutive days is just 1.0 psu, which occurred between Day 222 and Day 223 (August 10 and August 11). It is easily found from the local meteorological records that Shidao Observatory suffered from the Super Typhoon Lekima at those days. Meanwhile, because of longer rainy season, higher precipitation and more typhoon intrusions around Lianyungang Observatory compared with Shidao Observatory, the fluctuation of surface seawater salinity at Lianyungang Observatory of any two consecutive days is drastic, and obvious fluctuations over 1.0 psu are frequent. The maximum fluctuation of 8.4 psu occurred between Day 224 and Day 225 (August 12 and August 13), which was also affected by the Super Typhoon Lekima.

In summary, the marine hydrological data of Shidao Observatory and Lianyungang Observatory are reasonable and trustworthy. The measurand values are competent for further performance forecast of the proposed HPP-ERD.

Prior to the prediction calculation, there are three notes which should be clarified. The first is that the surface seawater temperatures measured at 8 am, 14 pm, and 20 pm are utilized to forecast the SEC from 0 am to 8 am, from 8 am to 16 pm, and from 16 am to 24 pm, respectively. The second is that the recorded surface seawater temperatures below 5.0 °C are taken as 5.0 °C because in practical SWRO projects, the feed seawater below 5.0 °C is usually heated to attain at least 5.0 °C to avoid the damage of RO membranes caused by low seawater temperature. The third is that, as a conservative precaution, the very few recorded surface seawater salinities below 21.0 psu are taken as 21.0 psu because the lower limit of salinity for regression is exactly 21.0 psu.

Economic calculations

The annual performance assessment of the proposed HPP-ERD focuses on both energy and economic aspects. The energy aspect is inspected simply by calculating the SEC through the regressed correlation formulas. The economic aspect is probed by calculating the annualized life cycle cost of fresh water. The monetary unit of RMB conveying primary economic data have been substituted by USD with a recent current exchange rate (1 USD = 6.34 RMB).

In agreement with the authors' previous work⁴⁶, the economic calculation of the proposed HPP-ERD incorporated with RO system is formulated conforming to the annualized life cycle cost method, which has been broadly recognized and employed for assorted types of desalination technologies^{52–57}. The annualized life cycle cost of fresh water (C_{fw}), which represents the economic performance, is calculated through the following equations:

$$CRF = \frac{i(1+i)^n}{(1+i)^n - 1} \quad (5)$$

$$AICC = ICC \times CRF \quad (6)$$

$$SFF = \frac{i}{(1+i)^n - 1} \quad (7)$$

$$ASV = SA \times SFF \quad (8)$$

$$AC = AICC + AMRC - ASV \quad (9)$$

$$C_{fw} = \frac{AC}{AQ_{fw}} \quad (10)$$

where CRF is the capital recovery factor, AICC is the annualized initial capital cost, ASV is the annualized salvage value, SA is the salvage value, SFF is the sinking fund factor, i is the interest rate, n is the lifespan, AC is the annualized cost, AMRC is the annualized maintenance and running cost, AQ_{fw} is the annualized fresh water productivity.

Systematically referring to the economic calculation and decision process of the authors' previous work⁴⁶, the conclusion given by Ziolkowska⁵⁸ that the parts cost can be presumed to be the same as membrane replacement cost, and a recent current exchange rate, the parameter values in Eqs. (5)–(10) can be easily obtained. The values of AICC and i are determined to be 79495 USD and 4.9%, respectively. Besides the electricity cost ($Cost_{ele}$), AMRC is comprised of annual chemical cost, annual membrane exchange cost and annual parts cost, which are assumed to be 848 USD, 791 USD and 791 USD, separately. The salvage value is taken to be 10% of the initial capital cost while the lifespan of the project is assumed to be 15 years. The annual electricity cost can be

obtained by:

$$\text{Cost}_{\text{ele}} = \sum_{\tau} Q_{\text{fw}} \times \text{SEC}_{\text{HPP-ERD}} + \text{SEC}_{\text{other}} \times C_{\text{ele}} \quad (11)$$

where τ denotes the certain time duration for the prediction of each day, Q_{fw} denotes the hourly fresh water productivity which is approximated as 1.96 m³ per hour, $\text{SEC}_{\text{HPP-ERD}}$ denotes the specific energy consumption of the proposed HPP-ERD derived from Eq. (4), $\text{SEC}_{\text{other}}$ denotes the specific energy consumption of other apparatus which is approximated as 1.0 kW-h per m³ complying with ref. ⁵⁹, C_{ele} denotes the electricity price which is approximated to be 0.08 USD per kilowatt-hour.

DATA AVAILABILITY

The data which support the current study are available from the corresponding author upon reasonable request.

Received: 8 February 2022; Accepted: 17 May 2022;

Published online: 07 June 2022

REFERENCES

- Okampo, E. J. & Nwulu, N. Optimisation of renewable energy powered reverse osmosis desalination systems: a state-of-the-art review. *Renew. Sustain. Energy Rev.* **140**, 110712 (2021).
- Soleimanzade, M. A. & Sadrzadeh, M. Deep learning-based energy management of a hybrid photovoltaic-reverse osmosis-pressure retarded osmosis system. *Appl. Energy* **293**, 116959 (2021).
- Fan, Q. et al. The role of micro-nano pores in interfacial solar evaporation systems – a review. *Appl. Energy* **292**, 116871 (2021).
- Lord, J. et al. Global potential for harvesting drinking water from air using solar energy. *Nature* **598**, 611–617 (2021).
- Habib, S. & Weinman, S. T. A review on the synthesis of fully aromatic polyamide reverse osmosis membranes. *Desalination* **502**, 114939 (2021).
- Feria-Díaz, J. J., Correa-Mahecha, F., López-Méndez, M. C., Rodríguez-Miranda, J. P. & Barrera-Rojas, J. Recent desalination technologies by hybridization and integration with reverse osmosis: a review. *Water* **13**, 1369 (2021).
- Lim, Y. J., Goh, K., Kurihara, M. & Wang, R. Seawater desalination by reverse osmosis: Current development and future challenges in membrane fabrication – a review. *J. Memb. Sci.* **629**, 119292 (2021).
- Shahzad, M. W., Burhan, M. & Ng, K. C. A standard primary energy approach for comparing desalination processes. *npj Clean Water* **2**, 1–7 (2019).
- Mito, M. T., Ma, X., Albuflasa, H. & Davies, P. A. Reverse osmosis (RO) membrane desalination driven by wind and solar photovoltaic (PV) energy: State of the art and challenges for large-scale implementation. *Renew. Sustain. Energy Rev.* **112**, 669–685 (2019).
- Kim, J., Park, K., Yang, D. R. & Hong, S. A comprehensive review of energy consumption of seawater reverse osmosis desalination plants. *Appl. Energy* **254**, 113652 (2019).
- Zhao, D. L. et al. Emerging thin-film nanocomposite (TFN) membranes for reverse osmosis: a review. *Water Res.* **173**, 115557 (2020).
- Hailemariam, R. H. et al. Reverse osmosis membrane fabrication and modification technologies and future trends: a review. *Adv. Colloid Interface Sci.* **276**, 102100 (2020).
- Qasim, M., Badrelzaman, M., Darwish, N. N., Darwish, N. A. & Hilal, N. Reverse osmosis desalination: a state-of-the-art review. *Desalination* **459**, 59–104 (2019).
- Liang, K. et al. The research and application progress of the isobaric erd technique for swro desalination plant. *Desalin. Water Treat.* **202**, 14–26 (2020).
- Huang, B., Pu, K., Wu, P., Wu, D. & Leng, J. Design, selection and application of energy recovery device in seawater desalination: a review. *Energies* **13**, 4150 (2020).
- Nassrullah, H., Anis, S. F., Hashaikheh, R. & Hilal, N. Energy for desalination: a state-of-the-art review. *Desalination* **491**, 114569 (2020).
- Alhathal Alanezi, A., Altaee, A. & Sharif, A. O. The effect of energy recovery device and feed flow rate on the energy efficiency of reverse osmosis process. *Chem. Eng. Res. Des.* **158**, 12–23 (2020).
- Im, S. J., Jeong, S. & Jang, A. Forward osmosis (FO)-reverse osmosis (RO) hybrid process incorporated with hollow fiber FO. *npj Clean Water* **4**, 51 (2021).
- Kim, Y., Kang, M. G., Lee, S., Jeon, S. G. & Choi, J. S. Reduction of energy consumption in seawater reverse osmosis desalination pilot plant by using energy recovery devices. *Desalin. Water Treat.* **51**, 766–771 (2013).
- Peñate, B. & García-Rodríguez Lourdes, L. Energy optimisation of existing SWRO (seawater reverse osmosis) plants with ERT (energy recovery turbines): technical and thermoeconomic assessment. *Energy* **36**, 613–626 (2011).
- El-Sayed, T. A. & Abdel Fatah, A. A. Performance of hydraulic turbocharger integrated with hydraulic energy management in SWRO desalination plants. *Desalination* **379**, 85–92 (2016).
- Stover, R. L. Seawater reverse osmosis with isobaric energy recovery devices. *Desalination* **203**, 168–175 (2007).
- Cameron, I. B. & Clemente, R. B. SWRO with ERI's PX Pressure Exchanger device - a global survey. *Desalination* **221**, 136–142 (2008).
- Eshoul, N. M., Agnew, B., Al-Weshahi, M. A. & Atab, M. S. Exergy analysis of a two-pass Reverse Osmosis (RO) desalination unit with and without an energy recovery turbine (ERT) and pressure exchanger (PX). *Energies* **8**, 6910–6925 (2015).
- Arenas Urrea, S., Díaz Reyes, F., Peñate Suárez, B. & de la Fuente Bencomo, J. A. Technical review, evaluation and efficiency of energy recovery devices installed in the Canary Islands desalination plants. *Desalination* **450**, 54–63 (2019).
- Pikalov, V., Arrieta, S., Jones, A. T. & Mamo, J. Demonstration of an energy recovery device well suited for modular community-based seawater desalination systems: Result of Danfoss iSAVE 21 testing. *Desalin. Water Treat.* **51**, 4694–4698 (2013).
- Peñate, B., de la Fuente, J. A. & Barreto, M. Operation of the RO Kinetic® energy recovery system: description and real experiences. *Desalination* **252**, 179–185 (2010).
- Song, J., Li, T., Wright-Contreras, L. & Law, A. W. K. A review of the current status of small-scale seawater reverse osmosis desalination. *Water Int.* **42**, 618–631 (2017).
- Chu, K. H. et al. Operational strategies for brackish water desalination plants in island regions of South Korea. *J. Clean. Prod.* **278**, 123540 (2021).
- Choi, J. S., Lee, S., Kim, J. M. & Choi, S. Small-scale desalination plants in Korea: Technical challenges. *Desalination* **247**, 222–232 (2009).
- Valbjørn, A. ERD for small SWRO plants. *Desalination* **248**, 636–641 (2009).
- Drablos, L. S. Testing of DanfossAPP1.0-2.2 with APP pumps as water hydraulic motors for energy recovery. *Desalination* **183**, 41–54 (2005).
- Dimitriou, E., Mohamed, E. S., Karavas, C. & Papadakis, G. Experimental comparison of the performance of two reverse osmosis desalination units equipped with different energy recovery devices. *Desalin. Water Treat.* **55**, 3019–3026 (2015).
- Thomson, M., Miranda, M. S. & Infield, D. A small-scale seawater reverse-osmosis system with excellent energy efficiency over a wide operating range. *Desalination* **153**, 229–236 (2003).
- Thomson, M. & Infield, D. Laboratory demonstration of a photovoltaic-powered seawater reverse-osmosis system without batteries. *Desalination* **183**, 105–111 (2005).
- Mohamed, E. S., Papadakis, G., Mathioulakis, E. & Belessiotis, V. The effect of hydraulic energy recovery in a small sea water reverse osmosis desalination system; experimental and economical evaluation. *Desalination* **184**, 241–246 (2005).
- Lu, Y., Zhao, Y., Bu, G. & Shu, P. The integration of water vane pump and hydraulic vane motor for a small desalination system. *Desalination* **276**, 60–65 (2011).
- Tian, J., Wang, Y., Zhou, J., He, Z. & Xu, S. Development and experimental evaluation of an innovative self-boosting energy recovery device for small-scale swro system. *Desalin. Water Treat.* **182**, 28–37 (2020).
- Sun, Z., Wang, Y., Zhou, J., Xu, Z. & Xu, S. Development and operational stability evaluation of new three-cylinder energy recovery device for SWRO desalination system. *Desalination* **502**, 114909 (2021).
- Zhou, J., Wang, Y., Duan, Y., Tian, J. & Xu, S. Capacity flexibility evaluation of a reciprocating-switcher energy recovery device for SWRO desalination system. *Desalination* **416**, 45–53 (2017).
- Schneider, B. Selection, operation and control of a work exchanger energy recovery system based on the Singapore project. *Desalination* **184**, 197–210 (2005).
- Mambretti, S., Orsi, E., Gagliardi, S. & Stover, R. Behaviour of energy recovery devices in unsteady flow conditions and application in the modelling of the Hama desalination plant. *Desalination* **238**, 233–245 (2009).
- Villa Sallangos, O. L. Operating experience of the Dhekiala seawater desalination plant using an innovative energy recovery system. *Desalination* **173**, 91–102 (2005).
- Koutsou, C. P., Kritikos, E., Karabelas, A. J. & Kostoglou, M. Analysis of temperature effects on the specific energy consumption in reverse osmosis desalination processes. *Desalination* **476**, 114213 (2020).
- Farooque, A. M. et al. Parametric analyses of energy consumption and losses in SWCC SWRO plants utilizing energy recovery devices. *Desalination* **219**, 137–159 (2008).
- Song, D. et al. Demonstration of a piston type integrated high pressure pump-energy recovery device for reverse osmosis desalination system. *Desalination* **507**, 115033 (2021).

47. Alkhadra, M. A., Gao, T., Conforti, K. M., Tian, H. & Bazant, M. Z. Small-scale desalination of seawater by shock electro dialysis. *Desalination* **476**, 114219 (2020).
48. ZHAO, J. et al. Review of cylinder block/valve plate interface in axial piston pumps: Theoretical models, experimental investigations, and optimal design. *Chin. J. Aeronaut.* **34**, 111–134 (2021).
49. Sun, J., Wang, Y., Xu, S., Wang, S. & Wang, Y. Performance prediction of hydraulic energy recovery (HER) device with novel mechanics for small-scale SWRO desalination system. *Desalination* **249**, 667–671 (2009).
50. Christopoulos, K., Pospotikis, N., Kostopoulos, E., Kondili, E. & Kaldellis, J. K. Experimental analysis of the water salinity impact on the energy consumption of small desalination plants. *Procedia Struct. Integr.* **10**, 171–178 (2018).
51. Ng, K. C. et al. A thermodynamic platform for evaluating the energy efficiency of combined power generation and desalination plants. *npj Clean Water* **4**, 1–10 (2021).
52. Liponi, A., Wieland, C. & Baccioli, A. Multi-effect distillation plants for small-scale seawater desalination: thermodynamic and economic improvement. *Energy Convers. Manag.* **205**, 112337 (2020).
53. Alhazmy, M. M. Economic and thermal feasibility of multi stage flash desalination plant with brine-feed mixing and cooling. *Energy* **76**, 1029–1035 (2014).
54. Bilton, A. M., Wiesman, R., Arif, A. F. M., Zubair, S. M. & Dubowsky, S. On the feasibility of community-scale photovoltaic-powered reverse osmosis desalination systems for remote locations. *Renew. Energy* **36**, 3246–3256 (2011).
55. Valladares Linares, R. et al. Life cycle cost of a hybrid forward osmosis - low pressure reverse osmosis system for seawater desalination and wastewater recovery. *Water Res.* **88**, 225–234 (2016).
56. Kabeel, A. E., Hamed, A. M. & El-Agouz, S. A. Cost analysis of different solar still configurations. *Energy* **35**, 2901–2908 (2010).
57. Zhang, Y., Zhang, H., Zheng, W., You, S. & Wang, Y. Numerical investigation of a humidification-dehumidification desalination system driven by heat pump. *Energy Convers. Manag.* **180**, 641–653 (2019).
58. Ziolkowska, J. R. Is desalination affordable?—regional cost and price analysis. *Water Resour. Manag.* **29**, 1385–1397 (2015).
59. Voutchkov, N. Energy use for membrane seawater desalination – current status and trends. *Desalination* **431**, 2–14 (2018).

ACKNOWLEDGEMENTS

The financial support from the Natural Science Foundation of Tianjin (No. 20JCZDJC00460), the Special Fund for Basic Scientific Research Business of Central Public Research Institutes (No. K-JBYWF-2021-QR04, No. K-JBYWF-2019-ZD01, No. K-JBYWF-2021-T07, K-JBYWF-2019-19), the Tianjin Science and Technology Program (No. 20YDTPJC00970), the Ministry of Industry and Information Technology (Document No. 357[2019]), and the Tianjin Technology Innovation Center

Construction Project is deeply appreciated. Special thanks to the National Marine Data Center, National Science & Technology Resource Sharing Service Platform of China (<http://mds.nmdis.org.cn/>) for its public marine hydrological data. Special thanks to Professor Shenghui Wang who gave us precious suggestions and guidance during our research, manuscript draft and submission processes.

AUTHOR CONTRIBUTIONS

Y.Z. made the economic calculation and wrote the original manuscript. D.S. supervised the research and analyzed the experimental data. H.W. and J.Z. established the experiment platform. X.W. and L.J. conducted the experiments. C.W. revised the manuscript. M.F. plotted the figures.

COMPETING INTERESTS

The authors declare no competing interests.

ADDITIONAL INFORMATION

Correspondence and requests for materials should be addressed to Daiwang Song.

Reprints and permission information is available at <http://www.nature.com/reprints>

Publisher's note Springer Nature remains neutral with regard to jurisdictional claims in published maps and institutional affiliations.



Open Access This article is licensed under a Creative Commons Attribution 4.0 International License, which permits use, sharing, adaptation, distribution and reproduction in any medium or format, as long as you give appropriate credit to the original author(s) and the source, provide a link to the Creative Commons license, and indicate if changes were made. The images or other third party material in this article are included in the article's Creative Commons license, unless indicated otherwise in a credit line to the material. If material is not included in the article's Creative Commons license and your intended use is not permitted by statutory regulation or exceeds the permitted use, you will need to obtain permission directly from the copyright holder. To view a copy of this license, visit <http://creativecommons.org/licenses/by/4.0/>.

© The Author(s) 2022